

The stress distribution in the whole area of the slab changed completely after the 2004 off Kii Peninsula earthquake

MASE, Hirofumi^{1*}

¹none

(Please refer to the figure. Names of the slab, topography of seabed, etc are naming only of here.)

In (1), the relation between the 2004 off Kii Peninsula earthquake and the 1944 Tonankai earthquake was researched. Mantle that heads eastward in the Chugoku region pushes the edge of the Nankai slab. The slab is placed between the right-turning force and the reaction from the south of the Trough. There are two Seamounts that resist in the south of the Trough and the reaction-stresses concentrate in those. After the north side of the Seamounts was destroyed by the earthquake in 2004, the route that power is transmitted to the Seamounts converted from "from North" to "from Northwest".

In (2), I searched for the evidence of the right-turn-force by using the focal mechanisms of earthquakes occurred on the surface of the Nankai slab and in it.

Because earthquakes that those compression axes and tangent of (circular arc)ar1-ar5 of which center of gyration is the south of Kii Suido harmonize are widely distributed, it turned out that power to induce the overall right-turn of the Nankai slab exists widely in each place.

I want to report on the result achieved by integrating (1) and (2).

The block arrows in Fig. 2 are average compression axial directions of the earthquakes that occurred in each area of the Nankai Slab obtained by (2). The compression powers to push the edge are transmitted in the slab and get to the Seamounts in which stress concentrate and to others. I expressed the typical transmission routes by A2,B2,C2,D2(arrows of short dashed line) following the block arrows. All except A2 are "from North" compression routes connected directly with the Seamounts (Fig. 2). These routes converted those directions in 2004 in dramatic form. A2 and B2 were changed into A1 and B1 respectively and "from Northwest" compression routes were formed (Fig. 1). Because the hypocenter of 1944 and 3 aftershocks were in a row and it was connected with WM Seamount (Fig. 1), it was able to be judged to be the compression route before 1944. The above is grounds of A1.

The outer of the right-rotation in 1944 traced the Crack(b) on inside from ar5 (4). Lateral-slip and collapse were generated because the transmission route until 1944 might have been C1,E1 (Fig. 1). Then, how did the transmission route after 1944 become? C1 curved to the west and changed into "from North" compression route C2,D2. And, E1 changed into the compression power that turns eastward like E2 (Fig. 2). I think certainly so.

Observation facts of (6) do not contradict the existence of the compression power shown by E2 before the earthquake in 2004. And they harmonize with the hypothesis that E2 was changed into the compression power shown by E1 after the earthquake.

Expectation in the future is as follows. After "from Northwest" compression continues for a while, the earthquake occurs and it returns to "from North" compression. This is the next Tonankai earthquake. The earthquake in 2004 was a halfway mark. If it was a literal midway point, this cycle is 120 years, and the remaining time is 50 years.

(1)MASE/Two seamounts in the near south of Nankai Trough concentrate stress like stake/JpGU2015/S-SS30/abstract submission

(2)MASE/Focal mechanisms prove the right-turn of slab beneath Kii Peninsula/JpGU2015/S-SS31/abstract submission

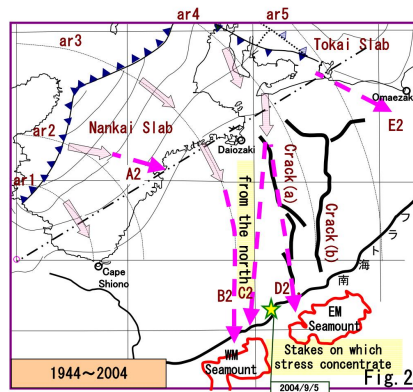
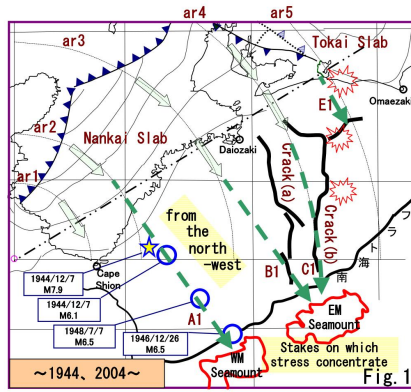
(4)MASE(2014)/JpGU2014/SSS29-P10

(6)Suito,Ozawa(2006)/<http://cais.gsi.go.jp/KAIHOU/report/kaihou77/12-1.pdf>

SSS27-P01

Room:Convention Hall

Time:May 24 18:15-19:30



/About sea bottom (shape line)
 extracted from (7)/
 /About "Nankai Slab" (shape line, contour) referable to (8)/
 /About "Tokai Slab" (shape line, contour) referable to (8)/
 /About information on earthquake referable to (10)/

Reference literature
 (5)木庭・巖谷(2005)/水準測量データの再検討による1994年東南海地震プレスリップ/名大
http://www.seis.nagoya-u.ac.jp/INTRO/report/jishinyochiren/162_kakegawa.pdf
 (6)水篠・小沢(2006)/12-1GPS連続観測から見た東海スロースリップ/GSI
<http://cais.gsi.go.jp/KAHOU/report/kaihou77/12-1.pdf>
 (7)JHOD/JCG/Seafloor Topography of the Plate Boundaries
http://www1.kaiho.mlit.go.jp/jishin/sokuryo_E/sokuryo_E.html
 (8)木村昌三(2001)/1946年南海地震に關係する四国における地震活動の特徴/(図2)
https://www.jstage.jst.go.jp/article/jgeography/1889/110/4/110_4_581/article-char/ja/
 (9)Nagoya Univ./Structure of the Subducting Philippine Sea Slab
<http://www.seis.nagoya-u.ac.jp/SEIS/slab/slab.html>
 (10)JMA/Monthly Report on Earthquakes and Volcanoes in Japan/September 2004/特集2/図7-1(P65)
<http://www.seisvol.kishou.go.jp/eq/gaiyo/index.html#monthly>

Predicting earthquakes just before by observing electric fields

TAKAHASHI, Kozo^{1*}

¹None

The precursory seismic electric fields will be generated by the mechanism as follows:

- (1) Before earthquakes, micro-cracks run in the source regions, and into these cracks pore water pours.
- (2) Uranium compounds, radium compounds and radon, which exist in crystal boundaries, dissolve into the pore water.
- (3) The cracks connect the pore water and spring water, and the radio active materials appear on the surface of source regions.
- (4) The active materials ionize the lower atmosphere above the source regions, and the electric conductivity increases there locally and temporarily.
- (5) The increase generates the current along the trace of cosmic shower between the surface and the ionosphere.
- (6) As the current is intermitting and pulsating, it radiates wide band radio-waves, which are observed as the precursory waves.

The occurrence of the precursory micro-cracks of the item (1) is indispensable, but is not yet observed, though the radio active materials of (3), the cloud caused by the current of (5) and the wide band radio-waves of (6) are already observed before big earthquakes. So, the above mechanism will be appropriate.

2. Mechanism generating the current of item (5),

The top of thunderclouds has the voltage up to about 100 MV, so the electrons and negative ions flow into the clouds from the ionosphere. As a result, the ionosphere has a few MV. The mechanism, which increases the voltage at the cloud top, will be as follows (Refer to figs):

(I) At middle latitudes, water drops in cumulonimbus change into ice crystals in the area where the temperature is about -10 deg. The melting temperature of a solid is lower on the surface than the inside, so at about -10 deg. the ice crystals are covered with liquid water film. The inside of the crystals there are free electrons and positive holes, and the electrons can move to the surface water, but the holes can't. So the water film is negatively charged, and the solid part of crystals positively charged. In the cloud, the crystals collide with each other, the collision is approximately elastic one where lower than -10 deg., and the change of speed of the smaller crystals is bigger than that of larger ones. Then the negative charge in the surface film on the smaller crystals moves to the larger crystal, and the smaller crystals become smaller and charged positive, are blown up to the cloud top, and make it high voltage. On the other hand, the larger crystals become larger, negative and drop down on the ground.

(II) At low latitude, in the cloud no water crystal will exist, but upward electric fields of about 1 kv/m exist, as at other areas. So, water drops are polarized such as the top is negative and bottom is positive. When they collide, the negative charge in the top of smaller water drops, which have higher speed than the larger ones, neutralizes the positive charge in the bottom of the larger water drops, and the smaller ones become positively charged and are blown up to the cloud top, resulting the high voltage.

(III) In the smoke billowing from volcanos, the lightning is observed, where cinders, ashes and blocks collide with each other, and are charged by frictional electricity. By the same reason shown in (II), the charge is polarized and high voltage in the upper part of the smoke is generated. As this high voltage is observed, the explanation mentioned above will be valid.

3. Earthquake prediction by observing electric fields

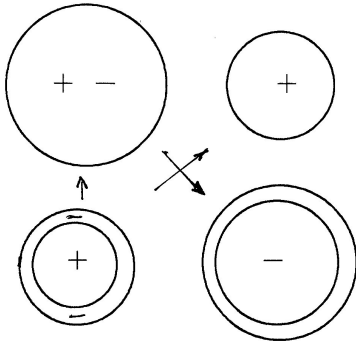
The site where the earthquakes occur will be the place where the electric fields are observed, because the fields will be generated at the place where the micro cracks generated. The magnitude will be estimated from the size of the area where the fields generate, because the magnitude is about proportional to the size of the area. About to the occurrence time, about one week before big earthquake occurrence the fields started to be observed.

Keywords: earthquake prediction, precursory seismic electric fields, mechanism of generating thunder, thunder in middle-latitude, thunder in low-latitude, thunder in smoke of volcano

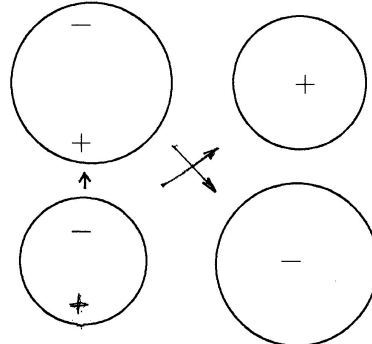
SSS27-P02

Room:Convention Hall

Time:May 24 18:15-19:30



At middle latitude



At low latitude

Long term predictability for the earthquake recurring a few times

TANAKA, Masayuki^{1*} ; OKADA, Masami¹ ; UCHIDA, Naoki²

¹Meteorological Research Institute, ²Graduate School of Science Tohoku University

Sequential recurrent large/medium earthquakes listed in seismic catalog are not so many, usually considerably few due to long return period, which are available to calculate the long term probability. We study the predictability for those cases using 127 sequences of small interplate repeating earthquakes along the Japan Trench which have been applied for an experiment of prospective forecast. Two to five events closely preceding forecast are picked from each sequence to calculate the probabilities for qualifying event in 2008.

We use three models to calculate the probabilities, as follow:

- (1) LN-Bayes: A Bayesian approach for lognormal distribution of recurrence interval with inverse gamma prior distribution. The parameters of inverse gamma are shape; $\phi=0.25$, and scale; $\zeta=0.44$.
- (2) LN-SST: Lognormal distribution model base on the small sample theory.
- (3) EXP-Pin: Exponential distribution model and the parameter being plugged in with the sample mean.

The "Mean log-likelihood" and "Brier score" mentioned below are used to score the forecast results.

Mean log-likelihood : Average of $E_v \cdot \log(P) + (1 - E_v) \cdot \log(1 - P)$

Brier score : Average of $(P - E_v)^2$

Here P means forecast probability for event and E_v means presence ($E_v=1$) or absence ($E_v=0$) of the qualifying event. The model is considered to be superior to the alternative one, if the Mean log-likelihood is larger and Brier score is smaller than those of the alternative, respectively.

Keywords: recurrent earthquake, forecast, Bayesian approach, Small sample theory, Mean log-likelihood, Brier score

Seismic quiescence and activation that precede large earthquakes and their source regions

YOSHIKAWA, Sumio^{1*} ; HAYASHIMOTO, Naoki² ; AKETAGAWA, Tamotsu³

¹MRI, ²MRI, ³OMO

The authors have attempted to detect and to quantify the quiescence phenomena of seismic activity prior to large earthquakes, by using an analyzing method of seismic quiescence and activation (eMAP). They have shown that there are scaling laws of quiescent area and lead-time with respect to earthquake magnitude, which suggests the possibility of earthquake forecasting in intermediate time scales (Yoshikawa et al., 2014). As it is necessary to improve the accuracy for application of this method to the forecast, we have investigated in details the relationship between seismic quiescence and activation that precedes a large earthquake and the source region.

Our past investigation for 26 major earthquakes with the magnitude larger or equal to 6.7 (focal depths less than 200km) has shown that 15 cases of quiescence can be retrospectively detected before the earthquake, and revealed that there is a proportionality between the relative source distance (the distance from the rupture point to the center of quiet region) and the size of the quiescent area (the major axis). In the present study, we investigated the relationship between the source regions of earthquakes and the quiescent and activated areas for the above 15 cases. According to the result there were 12 cases where the seismically quiescent area is surrounded or neighbored by the seismically activated areas, which has been called as the doughnut pattern (Mogi, 1969). The result indicates that in most cases quiescence can be more easily identified by co-existence of the activated areas. In almost all cases the quiescent area did not fit to the whole source region of a future earthquake, but it overlaps only with a part of it. That is, the quiescent area does not determine the future source region. However, we could find that there are at least 9 cases where a source region overlapped with one of seismically activated areas when the doughnut pattern was formed. This possibly suggests that to detect the doughnut pattern can contribute to estimate a future earthquake source region.

As pointed by Mogi (1979), the first kind seismic gap is defined as an unbroken part to be considered as asperity in a seismic zone, whereas the second kind seismic gap is defined as a part of temporary seismic quiescence. That the seismic quiescent area described above does not fit to the whole source region means that seismic quiescence is not caused in the asperity but caused by decrease in seismic activity due to aseismic slip in the fault surface. On the other hand, the seismic activation in surrounding of the quiescent areas may be caused by seismic activity in asperity.

Keywords: seismicity, quiescence, earthquake forecast

On the witness testimonies before the 1946 Nankai earthquake on the Pacific coast of Kii peninsula, Japan

UMEDA, Yasuhiro^{1*} ; ITABA, Satoshi¹

¹GSI, AIST

On the coast area of Kii peninsula, the witness testimonies before the 1946 Nankai earthquake were examined by literature surveys. Reduced or muddy well water has been witnessed in 14 locations. Sea level change has been witnessed in three locations. Land subsidence has also been reported, but it may also post-seismic phenomenon of 1944 Nankai earthquake.

Keywords: 1946 Nankai earthquake, witness testimony, well water, sea level change, land subsidence

Relation between tidal triggering effect and interplate seismicity along the Tonga-Kermadec trench

HIROSE, Fuyuki^{1*} ; KAMIGAICHI, Osamu² ; MAEDA, Kenji¹

¹Meteorological Research Institute, ²Japan Meteorological Agency

Tonga-Kermadec Trench is one of the world's most earthquake-prone zone. A convergence rate of plate increases from the south to the north and in proportion to it, seismicity rate is increasing [Ide, 2013, Nature Geo.]. In this area, larger earthquakes with $M \geq 7.5$ including intraplate earthquakes have most occurred around 1980 and 2010 relatively. About the former period, it was pointed out that p-value (Schuster, 1897, PRSL, it's an index to express correlation between the seismicity and the tide. Generally when it is less than 0.05, judged to the correlation is high significant) was lowered before Tonga earthquake in December 1982 (Mw7.5) and increased after the mainshock by Tanaka, et al. [2002, GRL], using the GCMT data from 1977 to 2000. About the latter period, the interplate earthquake (Mw7.6) has occurred in March 2009 near the 1982 earthquake.

In this study, we investigate the temporal variation of p-value before and after the mainshock in 2009 by using the GCMT data whose end period was extended to 2013. We target interplate earthquakes in the global CMT catalogue (rake angle is 60-120 degrees, depth is 0-70 km, strike angle is 150-230 degrees, the periods is 1977-2013). Theoretical tidal response in the crust is expressed as summation of the earth tide and ocean tidal loading effect. The former is calculated by "earthtide_mod" [Ozawa, 1974; Nakai, 1979; Kamigaichi, 2015, personal com.], the latter is calculated by the modified program [Kamigaichi, 1998, PMG; Kamigaichi, 2015, personal com.] based on "Gotic2" [Matsumoto, et al., 2001]. These programs use the PREM as an earth model in order to calculate the green function and output the strain tensor at the hypocenter of each events [Kamigaichi, 2015, personal com.]. We calculate delta CFF with the frictional coefficient is 0.4 on the fault plane from the strain tensor obtained. We set 50 events as the calculation unit in order to estimate the temporal variation of p-value and shifted them at every 1 event. The results are as follows.

- A. p-value decreases gradually before the 1982 mainshock and increases after that.
 - B. p-value decreases gradually (but at least 0.1) before the 2009 mainshock and increases after that.
 - C. There is five times of periods when p-value becomes less than 0.05 (Dec. 1982, Jan. 1988, Jun. 1993, Apr. 1998, Aug. 2000). However, about four times except for the mainshock in 1982, low p-value does not correspond large earthquakes with $M \geq 7.0$.
- A p-value is expected be an important tool for earthquake forecast because p-value decreases before large earthquakes and increases after them (e.g., 2004 Off Sumatra earthquake (Mw9.0) and its largest aftershock (Mw8.6), and 2011 Off Tohoku earthquake (Mw9.0) [Tanaka, et al., 2010, 2012, GRL]). However, if we conduct the earthquake forecast using temporal changes of p-value, we must take into account the false alarm such as "item C" above mentioned.

Keywords: Earth tide, Ocean tidal loading effect, delta CFF, p-value, Tonga-Kermadec trench